

# Study on Friction Stir Additive Manufacturing of Aluminium Alloys

A PROJECT REPORT

*Submitted in partial fulfillment of the  
requirements for the award of the degrees*

*of*  
**BACHELOR OF TECHNOLOGY**  
*in*

**MECHANICAL ENGINEERING**

*Submitted by:*  
**Gaurav Shukla**

*Guided by:*  
**Prof. N.K. Jain**



**INDIAN INSTITUTE OF TECHNOLOGY INDORE**  
**December 2019**



## **CANDIDATE'S DECLARATION**

We hereby declare that the project entitled “**study on friction stir additive manufacturing of aluminium alloys**” submitted in partial fulfillment for the award of the degree of Bachelor of Technology in ‘mechanical engineering’ completed under the supervision of **Prof. N.K. Jain, mechanical engineering, IIT Indore** is an authentic work.

Further, I/we declare that I/we have not submitted this work for the award of any other degree elsewhere.

**Signature and name of the student(s) with date**

---

## **CERTIFICATE by BTP Guide(s)**

It is certified that the above statement made by the students is correct to the best of my/our knowledge.

**Signature of BTP Guide(s) with dates and their designation**



## **Preface**

This report on “study on friction stir additive manufacturing of aluminium alloys” is prepared under the guidance of Prof. N.K. Jain.

Through this report I have tried to give detailed analysis of friction stir welding and friction stir powder additive manufacturing. In this report I have divided my study into two case studies to highlight the features of both processes separately. The case study 1 focusses on the influence of different process parameters on the properties of weld in friction stir welding while the case study 2 focusses on the quality of the deposition as well as the influence of rotational speed on different mechanical properties.

I have tried to the best of our ability and knowledge to explain the content in a lucid manner. I have also added figures and graphs to make it more illustrative.

**Gaurav Shukla**

B.Tech. IV Year

Discipline of mechanical engineering

IIT Indore



## **Acknowledgements**

I am immensely thankful to Prof. N.K. Jain for his patience, detailed critique of my work and kind encouragement while working on this project.

I am deeply indebted to research scholar Bhavesh Chaudhary for his assistance and support for this project through all phases of its development.

It is their guidance and support, due to which I became able to complete the experimental and technical report.

Without their support this report would not have been possible.

**Gaurav Shukla**

B.Tech. IV Year

Discipline of mechanical engineering

IIT Indore



## **Abstract**

The study focusses on the principal of friction stir additive processes and has been divided into two parts. The first case study highlights the characteristics of friction stir welding. It uses frictional heat as energy source to weld two base materials. It has brought great advancement in the field of welding dissimilar aluminium alloys because of its performance and efficiency. The two aluminium alloys, AA6061 and AA5083 are used for the experiment owing to their increasing application in aerospace industry. In order to fully understand and characterize the process, effect of various process parameters on the strength of weld has been studied by performing various tests namely, Vickers hardness test, tensile test and microstructure analysis. This case study is a preliminary analysis to understand the principals of friction stir processes.

The case study 2 concentrates on the characterization of deposition by friction stir powder additive manufacturing (FSPAM). This AM process uses similar principal as friction stir welding, utilizing frictional heat as a source of energy to soften the powder and deposits it on substrate. The aluminium alloy AA6061 and substrate of similar material are used to perform the experiments. The relationship between the rotational speed and various mechanical properties are established.



## Literature Review

A review of ongoing and completed research in the field of friction stir welding and friction stir powder additive manufacturing has been conducted to know the methodologies regarding the two processes.

Caizhi Zhou et al. investigated the fatigue properties of friction stir welds in Al 5083 alloy. They came to conclusion that fatigue life of friction stir welds were better than MIG-pulse welds and that all the cracks initiated from the root parts of the weld for all the fractured specimen.

H.W. Zhang et al. demonstrated the flow pattern using finite element simulation process by developing the two-dimensional model of FSW for an aluminium alloy to understand the mechanism of the process and the distribution of residual stresses. They were able to show that with increase in translational speed of the pin the maximum residual stress is increased and also that the material form fluidized bed around the pin on advancing side while no rotation of material on retreating side with the pin.

Jian-Qing Su et al. investigated the microstructural evolution during friction stir welding of high strength aluminium alloys. The research revealed different mechanism such discontinuous dynamic recrystallization, dislocation introduction, continuous dynamic recrystallization and dynamic recovery were the part of process at different stage and were responsible for refinement of microstructure in the stir zone.

Khalique Ejaz Ahmed et al. investigated the effect of rotational speed of the tool on friction stir welding of aluminium alloy 6082 with varying percentage of reinforcement of aluminium oxide. They were able to conclude that rotational speed influences the formation of defect, hardness as well as the tensile strength. They also showed that increase in the volume of reinforcement makes the weld more brittle.

Nirav P. Patel et al. developed the 3-D finite element based mathematical model to understand the temperature gradient in cooling assisted friction stir welding considering the material flow pattern of dissimilar Al-Cu joint.

B.J. Philips et al. studied the relationship between deformation and microstructure evolution in AA 6061 in additive friction stir process. They were able to show that slower deposit results in more recrystallized grain structure due to reduced strain and viscosity occurrence near the edge of tool and also concluded that dissolution of  $\beta''$  strengthening precipitates and re-precipitation of the Mg-Si solute cluster in the as deposited material.

O.G. Rivera introduced the new novel solid-state additive process known as additive friction stir and studied the microstructure and mechanical behavior of Inconel 625 fabricated by additive friction stir. It was the first manuscript which explained the mechanism behind the additive friction stir and revealed the presence of significantly refined grains localize to the interface layer.

# Table of Contents

Preface.....	5
Acknowledgements.....	7
Abstract.....	9
Literature Review.....	11
Table of Contents.....	13
List of Figures.....	15
List of Tables.....	17
Chapter 1. Friction Stir Welding.....	19
1.1. Introduction.....	19
1.1.1. Principle of friction stir welding.....	19
1.1.2. Microscopic Weld zones.....	20
1.1.3. Processing zones.....	20
1.1.4. Steps in FSW.....	22
1.2. Process Parameters.....	22
1.2.1. Transverse speed.....	23
1.2.2. Rotational speed.....	23
1.2.3. Coolant.....	23
1.2.4. Tool design.....	23
1.3. Experimentation.....	24
1.3.1. Objective.....	24
1.3.2. Material.....	24
1.3.3. Experimental Setup.....	24
1.3.4. Method.....	25
1.3.5. Sample preparation for characterization.....	25
1.4. Results and Discussions.....	27
1.4.1. Tensile Testing.....	27
1.4.2. Microstructure analysis.....	28
1.4.3. Micro-hardness Test.....	28
1.4.4. Effect of coolant on mechanical properties and microstructures.....	30

Chapter 2. Friction Stir Powder Additive Manufacturing .....	33
2.1. Introduction .....	33
2.1.1. Comparison between fusion based AM processes and friction stir AM processes. ....	33
2.1.2. Principal of FSPAM .....	34
2.2. Process Parameters .....	35
2.2.1. Rotational speed.....	35
2.2.2. Transverse speed.....	35
2.2.3. Tool design .....	35
2.3. Experimentation .....	36
2.3.1. Objective.....	36
2.3.2. Material.....	36
2.3.3. Experimental Setup.....	36
2.3.4. Method.....	38
2.3.5. Sample preparation for characterization .....	39
2.4. Results and Discussions .....	39
2.4.1. Calibration of powder feeder .....	39
2.4.2. Powder analysis .....	39
.....	40
2.4.3. Temperature variation.....	41
2.4.4 Micro-hardness Test .....	41
2.4.5. Microstructure analysis.....	43
2.4.6. Wear Test.....	44
2.4.7. Surface Roughness Test.....	47
Chapter 3. Conclusions.....	49
Chapter 4. Scope for Future Work.....	51
References.....	53

## List of Figures

Figure 1. Schematic of friction stir welding. ....	20
Figure 2. schematic representation of (a) weld zone and (b) processing zone. (Khan et al., 2018) .....	21
Figure 3. FSW tool design and dimensions. ....	21
Figure 4. Steps of FSW.....	22
Figure 5. Experimental setup for FSW. ....	25
Figure 6. Sample preparation, (a) cold mounting, (b) hot mounting and (c) tensile specimen. ....	26
Figure 7. Microscopic zones of FSW. ....	29
Figure 8. Graphical representation of micro-hardness of different weld zones.....	30
Figure 9. Comparison of microstructures of stir zone between forced cooling and natural cooling.....	32
Figure 10. (a) graph of comparison on accuracy and building rate between fusion based and friction stir based additive manufacturing, (b) comparison of capabilities between the fusion based and friction stir based AM process .....	34
Figure 11. Schematic of FSPAM.....	34
Figure 12. Tool shoulder geometry viewed from underneath the shoulder.....	36
Figure 13. Single pass deposition in FSPAM .....	37
Figure 14. Experimental setup for FSPAM .....	37
Figure 15. Sample preparation for characterization.....	38
Figure 16. Tool design used for FSPAM.....	38
Figure 17. EDX analysis of powder.....	39

Figure 18. Graphical representation of calibration of powder feeder.....	40
Figure 19. Temperature Profile at single point.....	41
Figure 20. Maximum temperature Vs rotational speed. ....	42
Figure 21. Graph of micro-hardness vs rpm.....	43
Figure 22. Comparison of microstructure between deposited layer and substrate. ....	43
Figure 23. Comparison of microstructure at different rotational speed.....	44
Figure 24. Height of deposition at different rotational speed. ....	44
Figure 25. Graphical representation of wear test.....	45
Figure 26. Coefficient of friction vs rotational speed.....	46
Figure 27. EDX analysis of wear track.....	46
Figure 28. SEM of wear track.....	46
Figure 29. Surface roughness vs rotational speed. ....	47

## List of Tables

Table 1. Properties of AA 6061 and AA 5083.....	24
Table 2. Design of experiments .....	27
Table 3. Tensile test of weld. ....	29
Table 4. Micro-hardness test.....	30
Table 5. Comparison of water-cooled and air-cooled deposition. ....	31
Table 6. Composition AA 6061-T6. ....	37
Table 7. Design of experiment.....	38
Table 8. Calibration of powder feeder. ....	40
Table 9. Vickers hardness test of FSPAM deposition. ....	42
Table 10. Fretting wear test. ....	45
Table 11. Surface roughness test. ....	47



# Chapter 1. Friction Stir Welding

## 1.1. Introduction

Friction stir welding is a relatively new solid-state welding process invented and patented by W.M. Thomas in 1991 at “TWI”, IN Cambridge, UK. It utilizes frictional heat developed between the tool and the base material as energy source to join material. The frictional heat softens the base material while the stirring action of the tool plasticizes it and the material flows around the tool in the form of plastic deformation to form the welded joint. The frictional heat was first utilized in friction welding where one of the two parts to be joined was rotated while the other remained stationary (Khan, Siddiquee, Khan, Bajaj, & Ubaid, 2018). The friction welding though being currently used is limited to cylindrical shapes in case of rotary friction welding and to rectangular shapes in case of linear frictional welding. Unlike friction welding, friction stir welding has a wider spectrum of shapes and many different configurations are possible using it.

Friction stir welding was initially developed to weld aluminium alloys (Dawes & Thomas, 1996), but due to its simplicity and efficiency its application was extended to other metal alloys such as copper, magnesium, steel, titanium, etc. Unlike conventional welding process no inert atmosphere and consumable tools are required in friction stir welding. It gained a major popularity after 1997 when Boeing adapted it for the fabrication of rocket fuel tank, wings, fuselages and carrier beams. Ship building industry and industrial sector are one of the major sectors presently utilizing friction stir welding to weld aluminium alloys.

### *1.1.1. Principle of friction stir welding*

The frictional stir welding uses frictional heat between the tool and the base material to softens the material but keeping the temperature below melting point of the two base materials. The temperature during welding is in the range of  $0.6 T_m - 0.9 T_m$ , where  $T_m$  is melting point of the base material (Mishra & Ma, 2005). The softened material plasticizes due to the stirring action of the tool and moves around the pin in the form of plastic deformation. The material moves from the advancing side of the tool to the retreating side and gets forged behind the tool by the shoulder to form the weld.

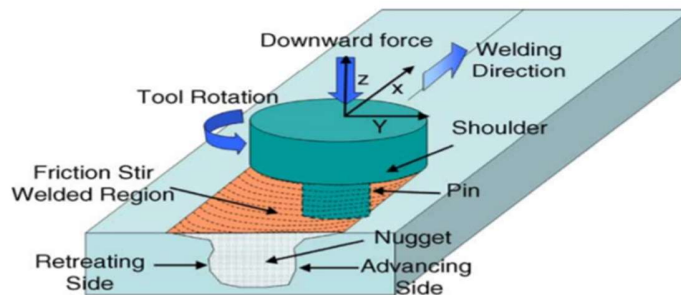


Figure 1. Schematic of friction stir welding.  
(Mishra and Ma, 2005)

### 1.1.2. Microscopic Weld zones

The microscopic investigation revealed the presence of different weld zones and these zones are classified based on the different mechanical and thermal cycle they undergo during welding. These zones are namely - weld nugget or stir zone (SZ), heat affected zone (HAZ), thermo-mechanically affected zone (TMAZ) and the base material (Feng, Wang, David, & Sklad, 2007) as shown in figure 2(a).

*Weld nugget:* This zone is the region where stirring takes place by the pin of the FSW tool. It is affected both mechanically and thermally by the tool and owing to which dynamic recrystallization takes place resulting in grain refinement.

*TMAZ:* This zone lies between the heat affected zone and weld nugget (weld nugget is a part of TMAZ). It experiences both deformation and thermal cycle but the intensity is reduced and therefore partial recrystallization occurs.

*HAZ:* This zone only experiences thermal cycle. It lies between the TMAZ and base material.

*BM:* It does not experience any kind of thermal or mechanical cycles during welding. And therefore, mechanical and thermal properties are not altered.

### 1.1.3. Processing zones

These zones in FSW explains the extrusion and forging process by the tool in the welding direction. Arbogast (Arbogast, 2006) classified friction stir welding process into five different

zone, namely – preheat zone, initial deformation zone, extrusion zone, forging zone and cooldown zone as shown in figure 2(b). The preheat zone is affected by the frictional heat developed but no plastic deformation occurs. The next zone in welding direction is initial deformation zone, it marks the initiation of plastic deformation during welding. Next is the extrusion zone, where the material moves around the pin from the advancing side to the retreating side undergoing severe plastic deformation and dynamic recrystallization. After the extrusion zone, forging takes place by the shoulder of the tool. The last zone is cool down zone where the forged material is cooled down to complete the weld.

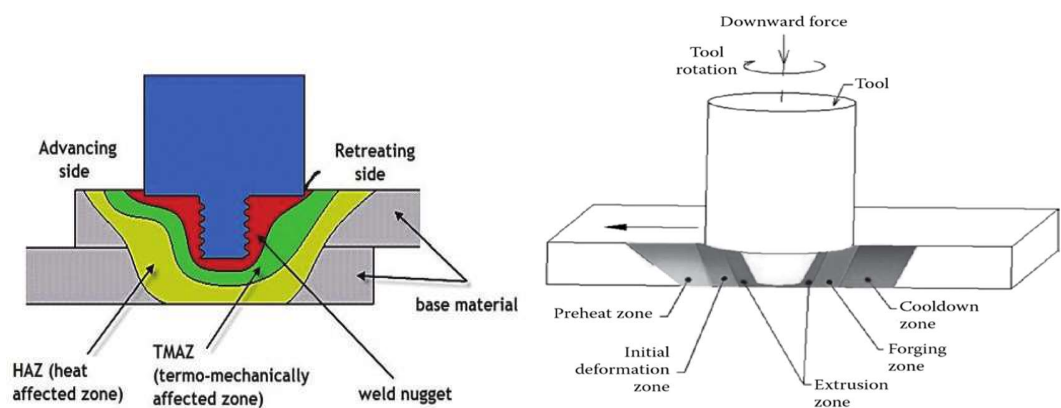


Figure 2. schematic representation of (a) weld zone and (b) processing zone. (Khan et al., 2018)

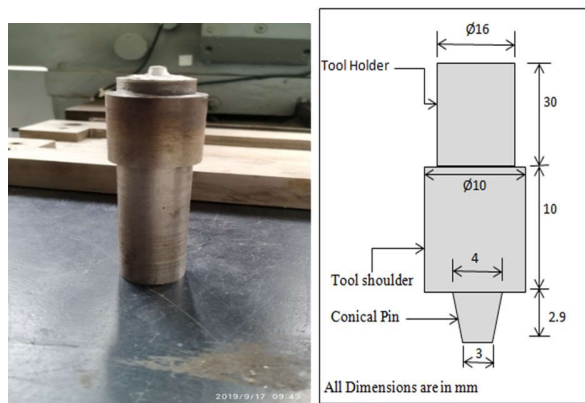


Figure 3. FSW tool design and dimensions.

#### 1.1.4. Steps in FSW

To weld two plates in FSW certain prescribe sequence should be followed. The sequence is divided into four phases namely, plunge phase, dwell phase, welding phase and retraction phase (Fraser, St-Georges, & Kiss, 2016).

In the plunge phase, the tool is rotated and plunged into the workpiece until the shoulder touches the workpiece. The workpiece is generally cold during this phase and therefore high force and torque are generated during this phase.

During the dwell phase, the rotation of tool generates heat due to relative motion between the workpiece and tool. The tool is rotated for a sufficiently long time to get to the temperature required for welding.

During the welding phase, the tool is allowed to move in transverse direction to form a weld. In the retraction phase the rotating tool is pulled out from the workpiece. At the end of retraction phase a circular cavity is left which should be removed or filled with the similar material.

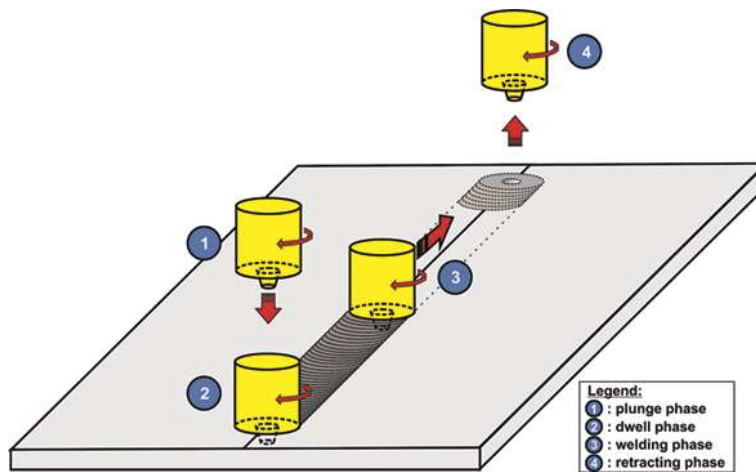


Figure 4. Steps of FSW.

(Fraser et al., 2016)

## 1.2. Process Parameters

Friction stir welding requires complex movement of material around the tool and therefore to understand this complexity various parameters such as tool transverse speed,

rotational speed, tilt angle, joint design, etc. should be studied to understand their impact on properties of weld.

#### *1.2.1. Transverse speed*

The transverse speed of tool is one of the most important parameters during welding as it affects the material flow along the length of weld. Increase in transverse speed reduces the peak temperature in the stirring zone due to lower energy input per unit weld length and also increases the possibilities of tunneling defects as increasing transverse speed reduces the consolidation behind tool pin. Due to lower heat input material flow around the pin is also affected.

#### *1.2.2. Rotational speed*

The rotational speed of the tool is the measure of the heat input to the weld, more the rotational speed more will be the heat input due to higher friction between the tool and the base material. The rotational speed of the tool is limited by the maximum force and torque produced during plunging phase. The relation between the heat input and the rotational speed is not monotonous as coefficient of friction between the tool and the workpiece depends on rotational speed (Mishra & Ma, 2005).

#### *1.2.3. Coolant*

The type of coolant is one of the deciding factors when it comes to weld quality. The coolant affects the grain structure of the weld and hence its properties. Generally, a better coolant provides better weld properties.

#### *1.2.4. Tool design*

The design of the tool decides the flow pattern as well as governs the force and torque produced. The tool in FSW consist of pin and shoulder and the size of shoulder relative to pin size plays important role in determining the heat input (Ni, Fu, Shen, & Liu, 2019). The shoulder features are used to increase heat input and reduce process loads.

## 1.3. Experimentation

### 1.3.1. Objective

The objective of this experiment is to study the effect of process parameters such as rotational speed, transverse speed and coolant, on the properties of the weld.

### 1.3.2. Material

The material opted for this experiment were two dissimilar aluminium alloy, AA 5083 and AA 6061. Due to large applications of combination of AA5083 and AA6061 in marine and aerospace industry, there has been a growing interest in the friction stir welding of above two aluminium alloys.

### 1.3.3. Experimental Setup

The experimental setup involves the use of vertical milling machine, non-consumable welding tool and plate fixture. The system monitoring control is used to set the transverse and rotational speed.

Table 1. Properties of AA 6061 and AA 5083

	AA 5083	AA 6061
Composition	Main component is magnesium with slight traces of manganese and chromium	Magnesium and silicon are its major alloying element
Properties	Non – heat treatable. Highly resistant to seawater corrosion	Heat treatable, high tensile strength, good weldability, easily extruded
Application	Ship building, rail cars, truck bodies, etc.	Aerospace structure, truck bodies, marine component, etc.

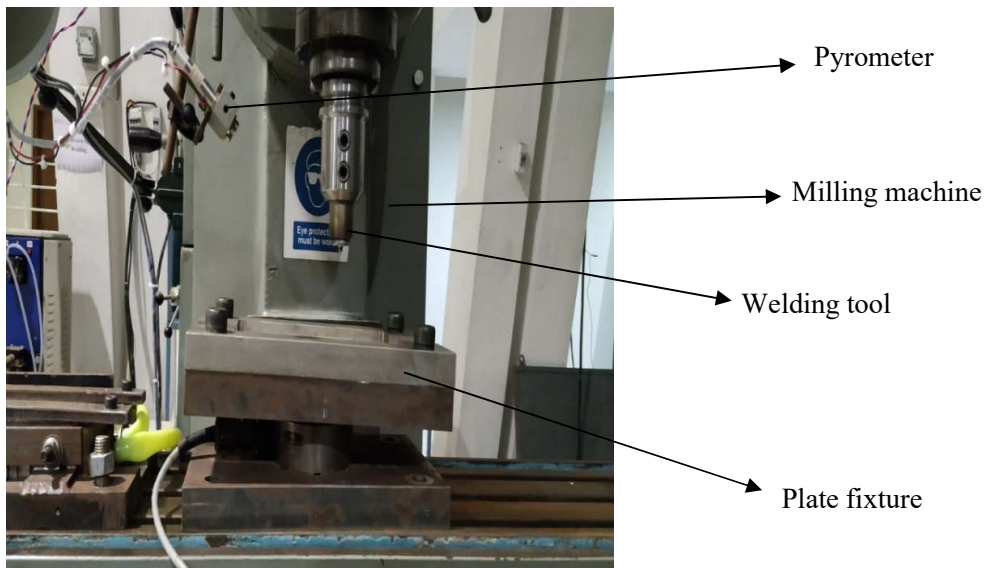


Figure 5. Experimental setup for FSW.

#### 1.3.4. Method

The two aluminium alloys were welded with a combination of three different rotational speed (900 rpm, 1000 rpm, 1200 rpm) and three transverse speed (40 mm/min, 50 mm/min, 60 mm/min). So, by using full factorial design total of 9 specimen were prepared. The sample with the maximum tensile strength was chosen for comparison with the water-cooled sample welded with same rotational and transverse speed. The sample number and the corresponding rotational and transverse speed are shown in table 2.

#### 1.3.5. Sample preparation for characterization

To determine the quality of weld, mechanical and microstructural characterization are required. They are useful in relating the process parameters to the performance of weld and in determining the failure behavior of joint. The microstructural investigation reveals the size, shape and orientation of grains and is also required to study the different microscopic weld zones.

Tensile testing was performed using UTM with the sample specimen as shown in figure 6(c). It was used to determine the ultimate tensile strength of the weld. Samples were prepared on EDM machine according to ASTM E8 standards. For optical microscopy and

micro-hardness polishing was required so the samples were first sectioned using wire electronic discharge machine and then were mounted for grinding. The mounting is required to maintain uniformity and for easy handling during grinding and are of two types- hot mounting and cold mounting. One sample was hot mounted while the others were cold mounted. The specimen after mounting was grinded using 200, 400, 600, 800, 1200,1500, 2000 grit silicon carbide paper to produce scratch free specimen. Next step was polishing, required to remove any scratches left and produce mirror polished surface using 1  $\mu\text{m}$  and 3  $\mu\text{m}$  diamond paste. Before the microscopic investigation of specimen, etchant was applied so as to get a clearer picture of microstructure. The etchant used in this experiment was Keller's etchant which consist of distilled water (190 mL), hydrofluoric acid (2 mL), hydrochloric acid (3 mL) and nitric acid (5 mL).



*Figure 6. Sample preparation, (a) cold mounting, (b) hot mounting and (c) tensile specimen.*

Table 2. Design of experiments

Experiment no.	Sample no.	Rotational speed (rpm)	Transverse speed (rpm)	Coolant
1	4	900	40	Air
2	9	900	50	Air
3	10	900	60	Air
4	3	1000	40	Air
5	6	1000	50	Air
6	8	1000	60	Air
7	2	1200	40	Air
8	7	1200	50	Air
9	5	1200	60	Air

Note: The sample no. 1 was water cooled sample and therefore was welded after welding the above 9 samples for comparison.

## 1.4. Results and Discussions

### 1.4.1. Tensile Testing

The tensile specimens were tested using ultimate tensile testing machine. The strength of weld depends on the metallurgical bonding between the two base materials which in this case takes place due to homogenous mixing and dynamic recrystallization of the two material. The higher rotational speed implies higher heat input while lower transverse speed also implies the same. The energy per unit weld length is given by the equation (W.J. Arbegast and P.J. Hartley, 1998): -

$$E = \frac{\omega\tau}{s} \quad \text{equation 1}$$

where  $\omega$  = angular velocity (radians/sec),  $\tau$  = pin tool torque (Nm),  $s$  = tool transverse speed (mm/sec) and  $\omega/s$  = heat ratio.

The high energy input implies higher plastic deformation and better flow of material around the pin but it also increases distortions and thus the strength can't be decide by the heat input

alone. (Khan et al., 2018). Therefore, no direct relation can be established between the tensile strength and heat ratio, even in the present experiments though it is observed that as we increased the  $\omega/s$  ratio tensile strength increased but we also have two different values of ultimate tensile strength at same heat ratio. The maximum tensile strength achieved was 225 MPa which was nearly 75% of one of the base materials (AA6061) which is higher when compared to conventional welding techniques. The specimen 4, 8, 9, 10 were not included for the tensile test because of visual defects present in them due to poor  $\omega/s$  ratio. The defects in them formed because of improper material flow due to poor combination of rotational and transverse speed.

#### *1.4.2. Microstructure analysis*

The microstructure analysis of the welded specimen of maximum tensile strength was investigated to recognize different zones formed during friction stir welding. The maximum tensile strength criteria was chosen because of the better material flow with least probability of defects. The three different zones namely TMAZ, HAZ and SZ were recognized as shown in figure 7. The grains of the SZ were finer compared to the other two zones and the base materials (AA 6061) as shown in figure 7. The finer equiaxed grains were formed as a result of dynamic recrystallization which occurred due to severe plastic deformation (Khan et al., 2018) and heat energy. The TMAZ has coarser grains compared to stir zone due to reduced intensity of thermal and mechanical cycle and as a result of which it is subjected to partial recrystallization. The HAZ has grain structure similar to base material as it is not affected by mechanical cycle but only by thermal cycle that too with reduced intensity when compared to stir zone and TMAZ. The mechanical properties are lowest in HAZ.

#### *1.4.3. Micro-hardness Test*

The microhardness test was performed using micro hardness testing machine UHL VHMT. The test was performed to understand the hardness variation across weld cross section and to know about the mechanical properties of different microscopic weld zones. The Vickers hardness test was performed under 50 gf with an indentation speed of 25  $\mu\text{m}/\text{sec}$  and dwell time of 15 sec. The results when plotted on graph followed a W-shaped curve as shown in figure 8. The hardness value of the stir zone was lower than the two base

material but was highest among other zones. This is may be due to finer grain structure compared to TMAZ and HAZ and it gets coarser as we move away from it. The hardness of the two-base material is higher despite having coarser grains due to the fact that lowering of hardness takes place during welding as the material get soften and also the dissolution of hardening precipitates which are responsible for hardness in base material takes place but some hardness in SZ is gained back as a result of dynamic recrystallization (Svensson and Karlsson, 1999).

Table 3. Tensile test of weld.

Experiment number	Rotational speed (rpm)	Transverse speed (mm/min)	Coolant	$\frac{\omega}{s}$	Tensile strength (MPA)
1	900	40	Air	22.5	-
2	900	50	Air	18	-
3	900	60	Air	15	-
4	1000	40	Air	25	195
5	1000	50	Air	20	213
6	1000	60	Air	16.67	-
7	1200	40	Air	30	225
8	1200	50	Air	24	168
9	1200	60	Air	20	188

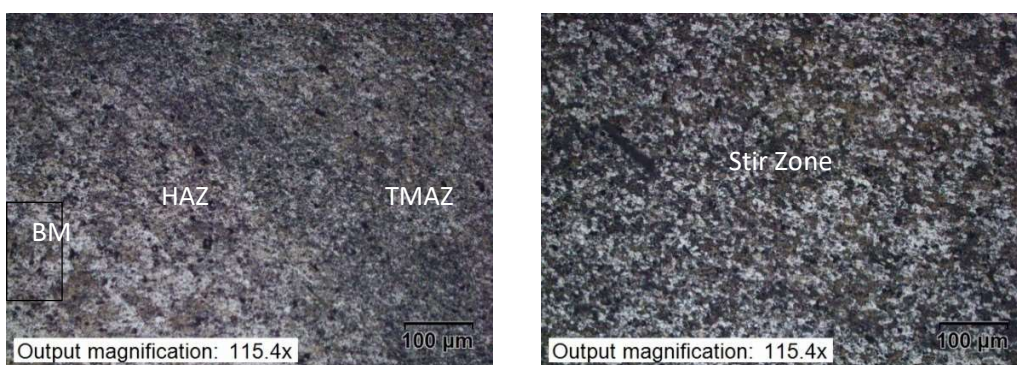


Figure 7. Microscopic zones of FSW.

Table 4. Micro-hardness test

-5	-4	-3	-2	-1	0	1	2	3	4	5
HV										
77	56	56	58	64	72	63	57	54	54	80

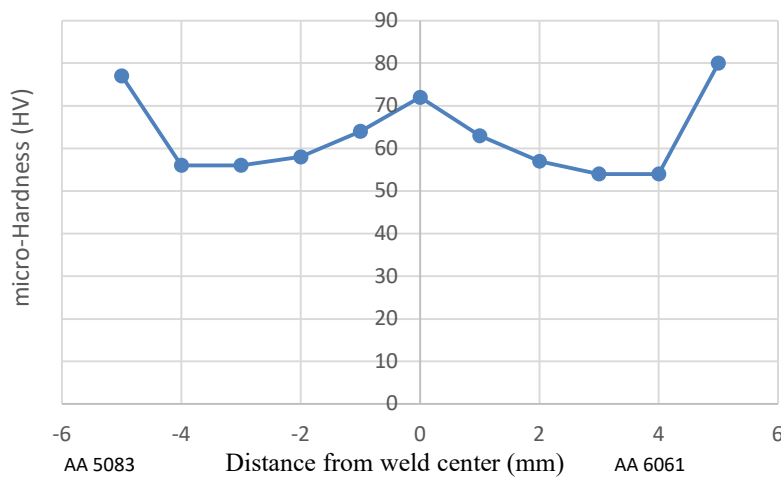


Figure 8. Graphical representation of micro-hardness of different weld zones

#### 1.4.4. Effect of coolant on mechanical properties and microstructures.

The property of coolant greatly affects the mechanical properties of weld as it influences the size of microstructure directly. The two coolant, air and water are compared based on three different properties of weld namely micro-hardness, tensile strength and the microstructures. The water as a coolant was used by using special fixture. The result shows that the increase in ultimate tensile strength due to forced cooling by water was roughly 4.5% of ultimate tensile strength of air-cooled sample. The increase in strength can be justified by two reasons, firstly the grains in the stir zone are finer and more homogenous in case of forced cooling and following the Hall-Petch equation, the strength will increase. Secondly the cooling kept the distortion low as the temperature profile was lower compared

to air cooled sample and hence, increase in strength (Peel, Steuwer, Preuss, & Withers, 2003).

$$\sigma_{yp} = \sigma_0 + \frac{k}{\sqrt{d}} \quad (\text{Hall-Petch equation}) \quad \text{equation 2}$$

Where  $\sigma_{yp}$  = yield stress,  $\sigma_0$  = friction stress, k = locking parameter and d = grain diameter.

The hardness value showed an increase of about 2.8% of micro-hardness value of air-cooled sample at the center of weld. This increase is because of better cooling rate in case of water and as a result restricting the growth of grains after dynamic recrystallization.

The grains were finer in case of forced cooling when compared to air-cooled weld. Water being a better coolant increases the cooling rate and therefore restricted the growth of grains during growth phase. The water as a coolant also reduced the distortion by keeping the temperature profile lower than the air-cooled sample.

*Table 5. Comparison of water-cooled and air-cooled deposition.*

Sample number	Coolant	Ultimate tensile strength (Mpa)	Strength in comparison to the base material (%)
2	Air	225	76
1	Water	235	80

Coolant	-5 (HV)	-4 (HV)	-3 (HV)	-2 (HV)	-1 (HV)	0 (HV)	1 (HV)	2 (HV)	3 (HV)	4 (HV)	5 (HV)
Air	77	56	56	58	64	72	63	57	54	54	80
Water	76	58	59	62	66	74	65	59	56	55	82

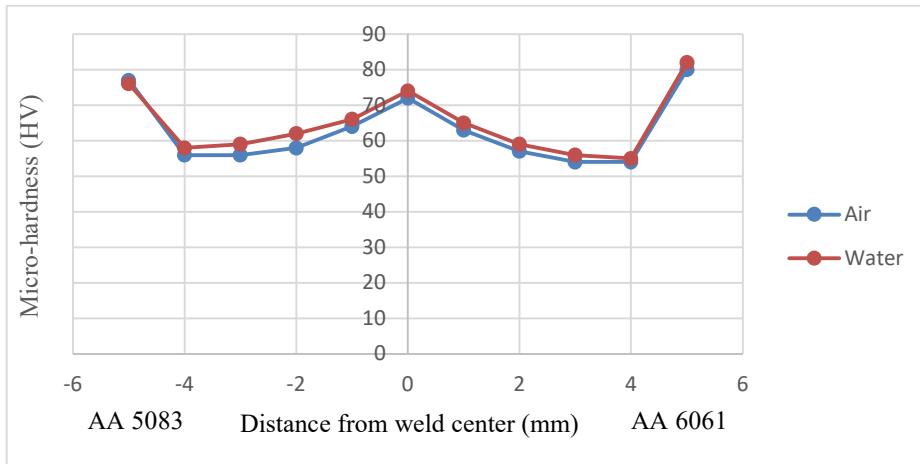


Figure 9. Graph of micro-hardness vs distance for water and air

Air-cooled



Water-cooled

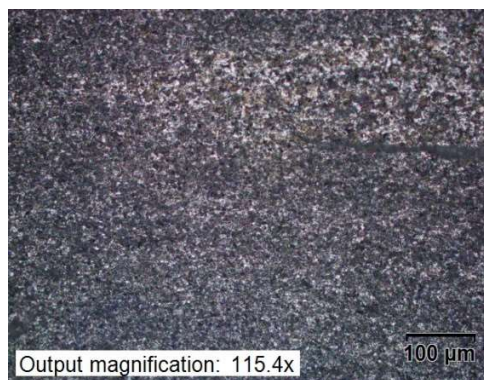


Figure 9. Comparison of microstructures of stir zone between forced cooling and natural cooling.

## Chapter 2. Friction Stir Powder Additive Manufacturing

### 2.1. Introduction

The friction stir powder additive manufacturing is an advanced solid state additive manufacturing process that utilizes frictional heat as energy source similar to friction stir welding energy to soften the material and plastically deform it. It fully adheres to the principle of layer by layer deposition of additive manufacturing process. The powder from a rotating non-consumable tool gets deposited on a substrate without any use of pin or probe. The manufactured parts possess wrought homogenous microstructural properties (Rathee, Srivastava, Maheshwari, Kundra, & Siddiquee, 2018). The grain refinement that occur due to dynamic recrystallization during deposition improves the mechanical properties of components. Presently friction stir powder additive manufacturing is being used in the fields of repairing substrate, coating substrate, stiffening and enhancing structures (Aeroprobe corporation) and also its use in fabricating components of metal matrix composites has been described (Khodabakhshi & Gerlich, 2018).

#### *2.1.1. Comparison between fusion based AM processes and friction stir AM processes.*

The friction stir based additive manufacturing gained popularity because of the absence of defects such as hot cracking, dilution, porosity, etc. which occur due to solidification of molten material in fusion based welding process. These defects influence the performance of components manufactured by fusion based processes such as powder bed fusion and direct energy deposition (Rivera et al., 2017). Although the structural performance of the component manufactured by FSPAM increases but the cost and resolution still remains a challenge for FSPAM as shown in figure 8 (Khodabakhshi & Gerlich, 2018). The material flow in FSPAM heal cracks and fill voids leading to good interfacial bonding and no observed porosity. There is low residual stresses and less distortion compared to fusion based process due to lower maximum temperature as no melting occurs.

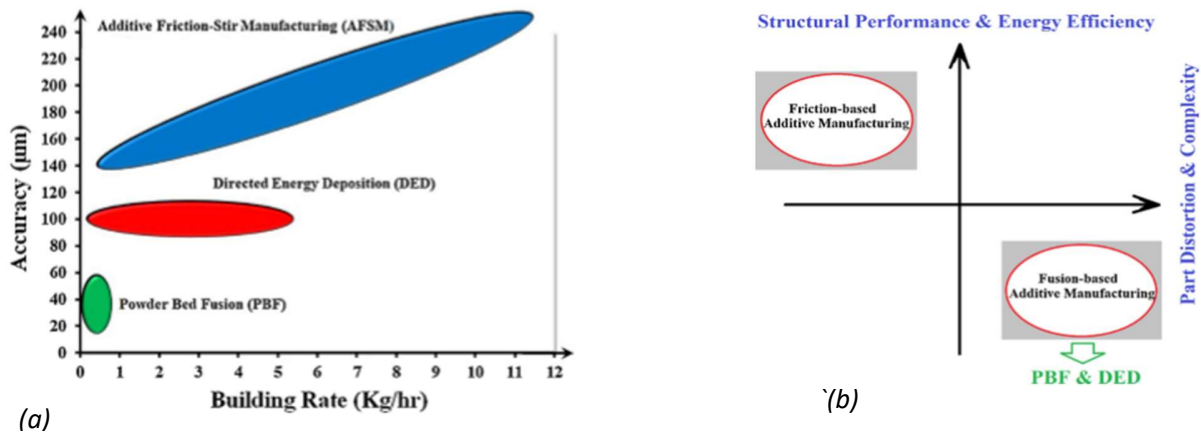


Figure 10. (a) graph of comparison on accuracy and building rate between fusion based and friction stir based additive manufacturing, (b) comparison of capabilities between the fusion based and friction stir based AM process (Khodabakhshi & Gerlich, 2018).

### 2.1.2. Principal of FSPAM

The FSPAM utilizes frictional heat produced between the tool and the powder and tool shoulder and substrate. It uses a hollow non consumable tool without pin or probe. The powdered material from powder flows through the rotating spindle and gets deposited on the substrate for the first layer while the subsequent layers are deposited on pre-deposited layer. For each layer tool height needs to be adjusted for the deposition on subsequent layer. The dynamic recrystallization due to heat energy and severe plastic deformation results in strong metallurgical bond between adjacent layer (Rivera et al., 2017). The finer, equiaxed grains and defect free microstructure after deposition imparts strength and toughness to the manufactured component.

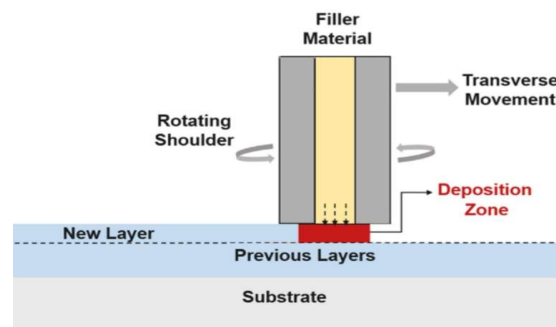


Figure 11. Schematic of FSPAM.

(<https://www.insidemetaladditivemanufacturing.com>)

## **2.2. Process Parameters**

Transverse speed, rotational speed, powder flow rate, tilt angle and tool design are some of the important parameters that influence the efficiency and performance of deposition.

### *2.2.1. Rotational speed*

The rotational speed has the main responsibility of producing heat and mixing the softened material, more the rotational speed more will be the heat energy input and hence temperature profile will be higher. The curve of heat energy input and rotational speed is not monotonous as the coefficient of friction between the tool and the base material depends on the rotational speed and many other external factors. The rotational speed of tool plastically deforms the softened powder and is stirred intensely which results in finer and homogenous grain structure.

### *2.2.2. Transverse speed*

The increase in transverse speed reduces the heat input per unit weld and therefore decreases the plastic deformation which in turn impacts the material flow around the tool and increase process load but it also helps in reducing the temperature profile owing to which distortion is reduced. The transverse speed is also related to building rate of component, higher the transverse speed faster will be the deposition and the building rate will be higher.

### *2.2.3. Tool design*

The tool performs two important functions, firstly it helps in generating majority amount of heat and secondly it mixes the softened powder to get a homogenous finer grain structure. The tool shoulder diameter relative to powder flow rate governs the mixing and deposition of the powdered material. Several tool shoulder feature for Friction stir welding has been devised that can be used for FSPAM for uniform deposition of the powder across the shoulder and lowering process loads.

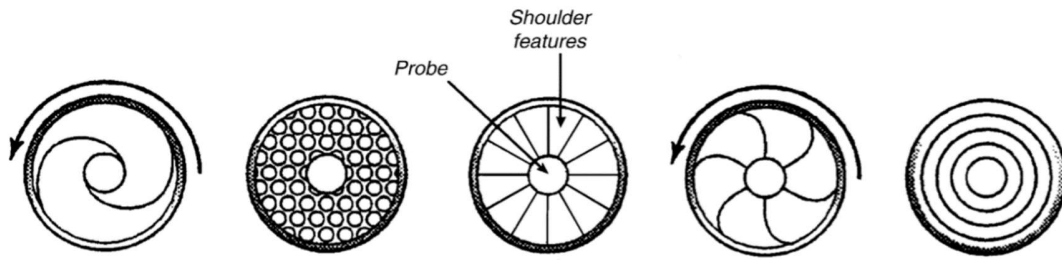


Figure 12. Tool shoulder geometry viewed from underneath the shoulder.

(Copyright© 2001, TWI Ltd) (Mishra & Ma, 2005)

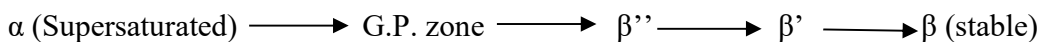
## 2.3. Experimentation

### 2.3.1. Objective

The object of this experiment analysis is to determine the quality of single-track deposition by FSPAM. In order to determine the quality, the dependence of mechanical properties on the tool rotational speed is explained.

### 2.3.2. Material

The material opted for this study was AA 6061 alloy. The composition of the AA 6061-T6 is given in table 6 (Mahto, Bhoje, Pal, Joshi, & Das, 2016). It is a precipitation hardened aluminium alloy with high strength and good weldability and is most commonly used in extrusion. The enhancement of strength by strengthening precipitates is achieved following the given phase reaction-



where  $\beta''$  and  $\beta'$  are metastable phase while  $\beta(\text{Mg}_2\text{Si})$  is a stable phase (Khan et al., 2018).

### 2.3.3. Experimental Setup

The experimental setup used in this experiment is shown in figure 13. The setup shown is similar to friction stir welding setup with only difference being the powder feeder which was mounted on the top of vertical milling machine. The load cell was used to measure the force during deposition and the single channel pyrometer was used to measure temperature profile at single point. The feed rate and rotational speed were being monitored

using computer and the data of the pyrometer and load cell was displayed on it. The voltage supplier was used to power powder feeder motor.

Table 6. Composition AA 6061-T6.

Al	Si	P	Mg	Ti	Cr	Mn	Fe	Cu	Zn
98.36	0.72	0.01	0.03	0.01	0.18	0.05	0.35	0.28	0.01

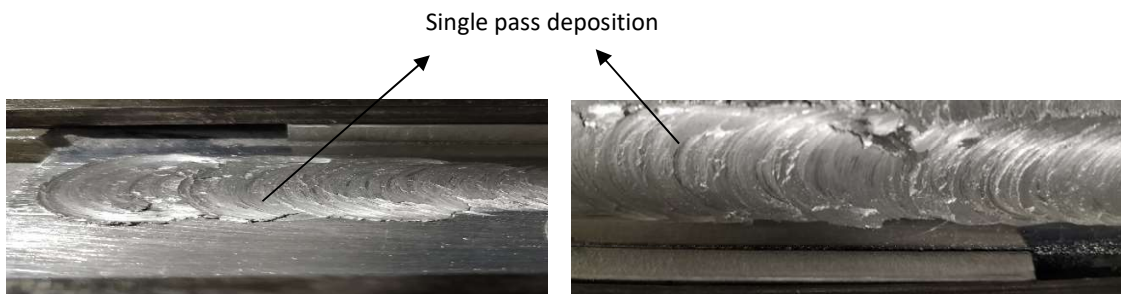


Figure 13. Single pass deposition in FSPAM

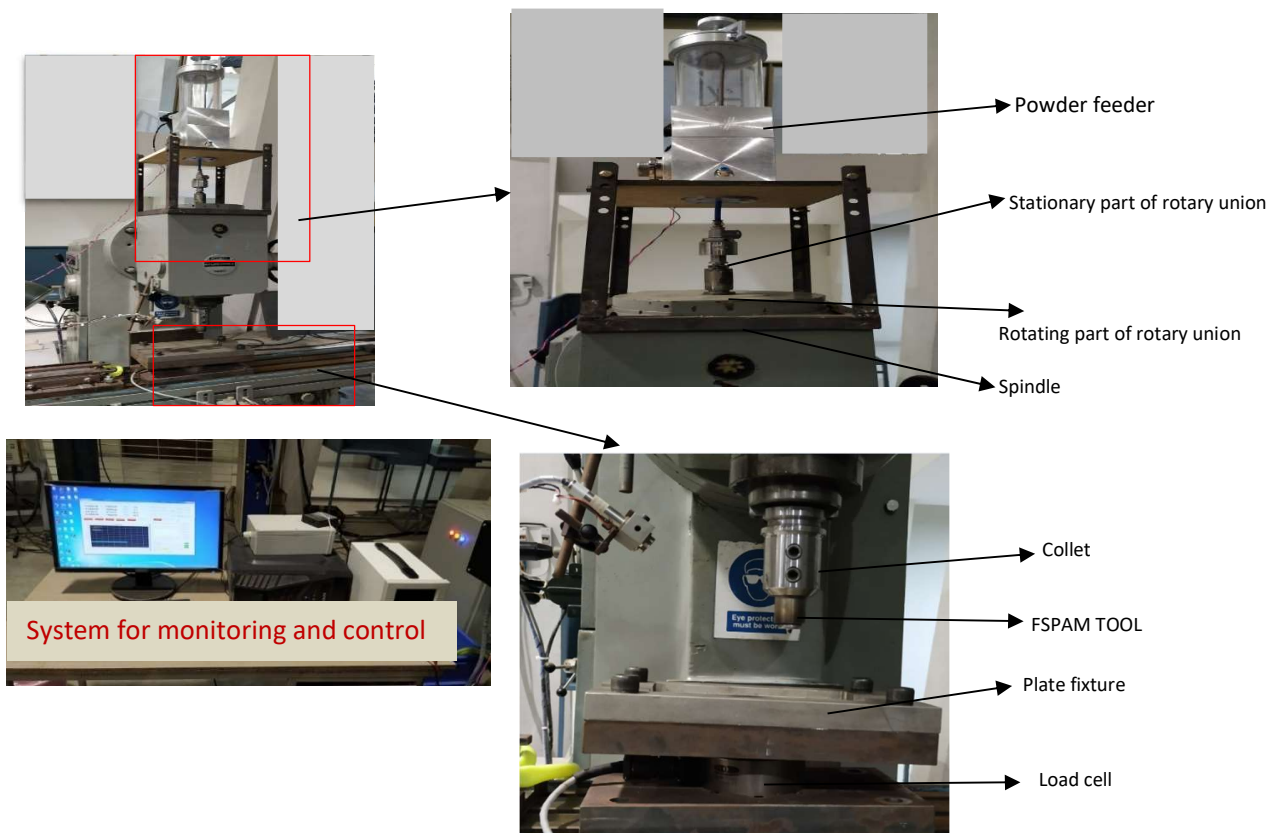


Figure 14. Experimental setup for FSPAM

#### 2.3.4. Method

The deposition was carried out at 5 different rotational speed – 600, 700, 800, 900, 1000 rpm at constant transverse speed of 15 mm/min and powder flow rate of 1500 mm<sup>3</sup>/min. All the depositions were carried out for single pass. To characterize the single pass deposition, Vickers micro-hardness test, microstructure analysis using optical microscopy, wear test, SEM of wear track and surface roughness test were performed.

Table 7. Design of experiment

Sample number	Rotational speed (rpm)	Feed rate (mm/min)	Powder flow rate (mm <sup>3</sup> /min)
1	600	15	1500
2	700	15	1500
3	800	15	1500
4	900	15	1500
5	1000	15	1500



Figure 15. Sample preparation for characterization.



Figure 16. Tool design used for FSPAM

### 2.3.5. Sample preparation for characterization

The samples from the cross section of deposition were cut to perform the test for characterization. They were hot mounted, grinded with grit paper of grades – 100, 200, 400, 800, 1000, 1200, 1500 and 2000. The samples were later polished with diamond paste to get a mirror like finish. The samples were then used for micro hardness test. For optical microscopy Keller’s reagent was applied to reveal grain boundaries. The samples for the wear test and surface roughness were cut in dimensions of 20 x 10 x 5 (mm).

## 2.4. Results and Discussions

### 2.4.1. Calibration of powder feeder

The powder feeder was calibrated prior to its use. The rotational speed of motor was related to the supply voltage and then the powder flow rate at various supply voltage was evaluated. The maximum powder flow rate of 1500 mm<sup>3</sup>/min was achieved at 22 V. The relation between the powder flow rate and supply voltage was not monotonous but the graph has a increasing trend as shown in figure 17 i.e., the powder flow rate increased with increasing supply voltage.

### 2.4.2. Powder analysis

The powder used for the experiment was analyzed before use in order to relate our results to aluminium alloy AA 6061. The powder was analyzed using energy dispersive x-ray technology (EDX). The powder had aluminium, magnesium, silicon with some impurities of calcium as shown by the peaks in figure 17(b). The size of grains of powder as evaluated from electron image varied from 50-100 micron as shown in figure 17(a).

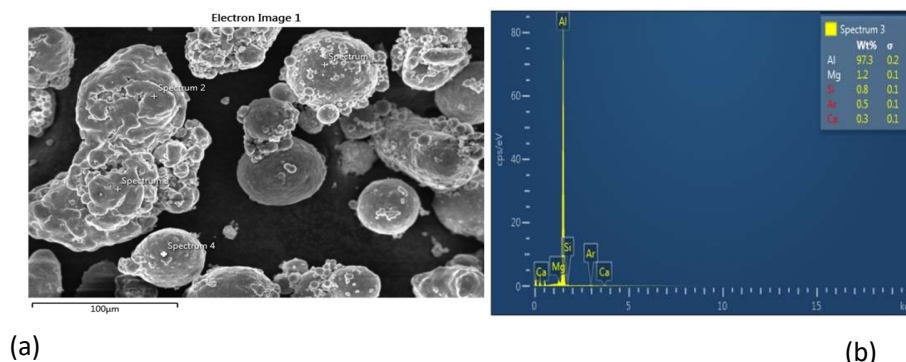


Figure 17. EDX analysis of powder.

Table 8. Calibration of powder feeder.

Exp. No	Gas flow rate (L/min)	Voltage (v)	Corresponding rpm (N)	Powder flow rate (g/min)
1	2	6	5.2	1
2	2	7	6.2	1.45
3	2	8	7.2	1.3
4	2	9	8.2	1.3
5	2	10	9.3	1.4
6	2	11	10.2	1.95
7	2	12	11.3	1.95
8	2	13	12.2	2.2
9	2	14	13.2	1.6
10	2	15	14.3	2.05
11	3	6	5.2	0.65
12	3	7	6.2	0.85
13	3	8	7.2	0.9
14	3	9	8.2	0.75
15	3	10	9.3	0.95
16	3	11	10.2	1.25
17	3	12	11.3	1.3
18	3	13	12.2	1.45
19	3	14	13.2	1.4
20	3	15	14.3	1.65
21	3	16	15.2	1.4
22	3	17	16.4	1.55
23	3	18	17.3	1.85
24	3	19	18.2	2.75
25	3	20	19.1	2.85
26	3	22	20.3	3.2
27	3	23	21.2	4.05
28	3	24	22.3	3.25

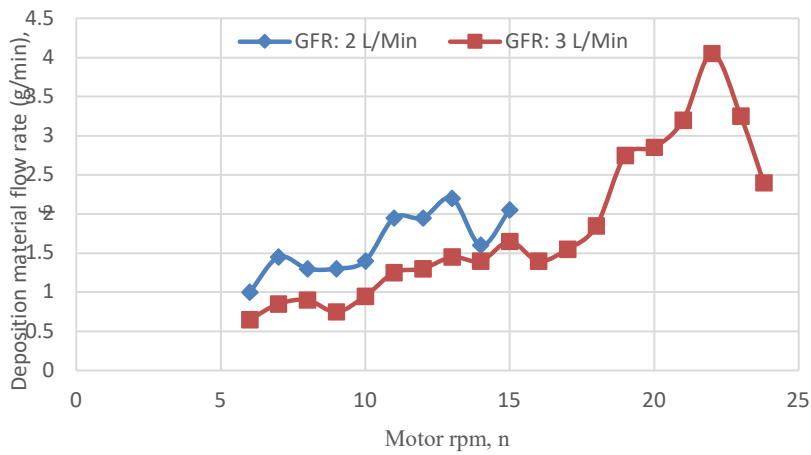


Figure 18. Graphical representation of calibration of powder feeder.

### 2.4.3. Temperature variation

The temperature variation was studied at a single point at the center of deposition. The peak was attained at the time when the tool reached the center of deposition i.e., the measuring point.

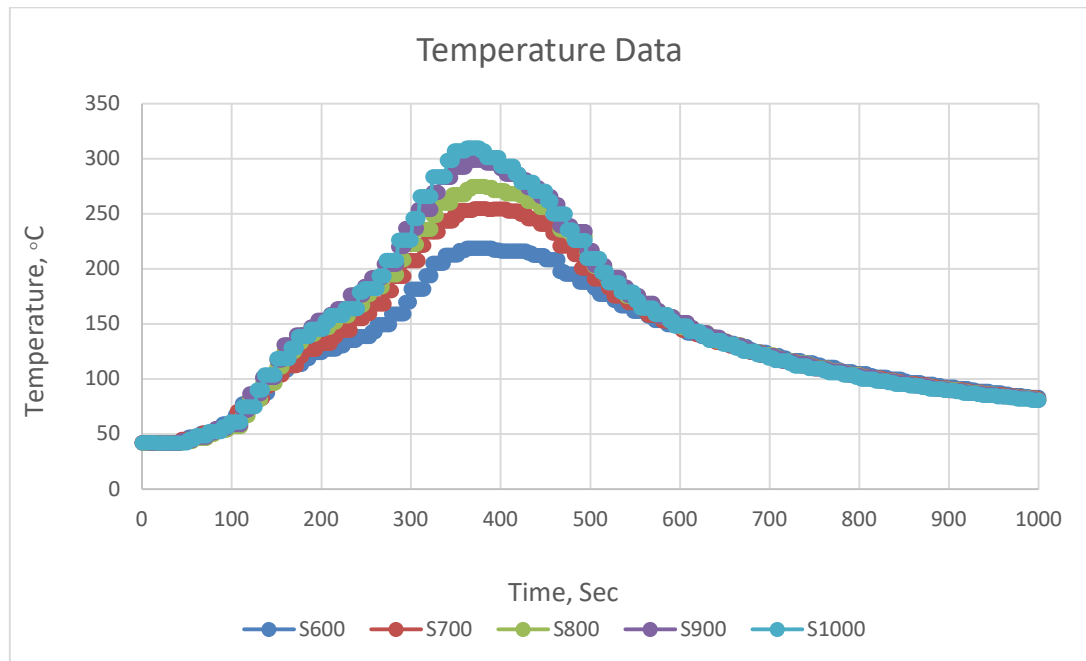


Figure 19. Temperature Profile at single point.

### 2.4.4 Micro-hardness Test

The micro-hardness of the deposited layer increased on decreasing rotational speed. The main reason behind the result was the increase in temperature profile with the increasing rotational speed and hence the increase in expansion growth rate of grains at elevated temperature. The variation of micro-hardness across the deposition height was also measured and it showed a decreasing trend as we moved away from the free surface toward the substrate. This result can be explained by a reason that the layer close to is not in direct contact with air (coolant) and hence the lower layer remains at elevated temperature for a longer time resulting in higher distortion and coarser grains.

Rotational speed (rpm)	600	700	800	900	1000
Maximum temperature (°C)	218.7	254.6	274.6	298.6	309.9

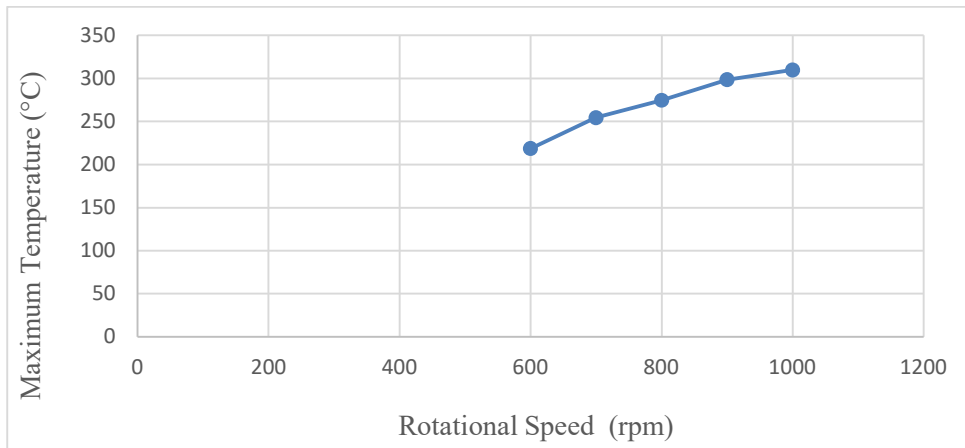


Figure 20. Maximum temperature Vs rotational speed.

Table 9. Vickers hardness test of FSPAM deposition.

Rotational Speed (rpm)	600 (HV)	700 (HV)	800 (HV)	900 (HV)	1000 (HV)
Deposition	160	134	103	89	67
↓	137	106	84	75	62
↓	96	87	66	53	44
Base Material	92	92	92	92	92

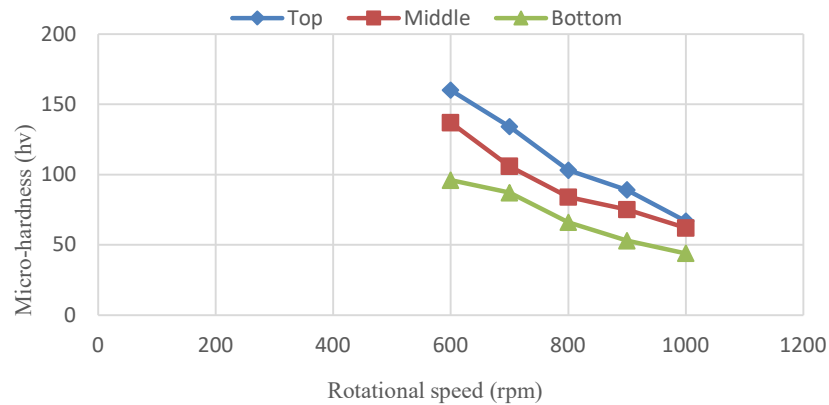


Figure 21. Graph of micro-hardness vs rpm

#### 2.4.5. Microstructure analysis

To determine the microstructure of the deposition and also to evaluate the deposition height for a single pass by FSPAM, the sample were grinded, polished and etched with Keller's reagent and viewed under optical microscopy. The grains of the deposition were finer compared to that of substrate (both substrate and powder was AA 6061) as shown in figure 19 due to dynamic recrystallization. The coarsening of grains in deposition region increased with increasing rotational speed as shown in figure 20, mainly because of the higher temperature profile which results in increase in distortion and expansion rate of grains at elevated temperature.

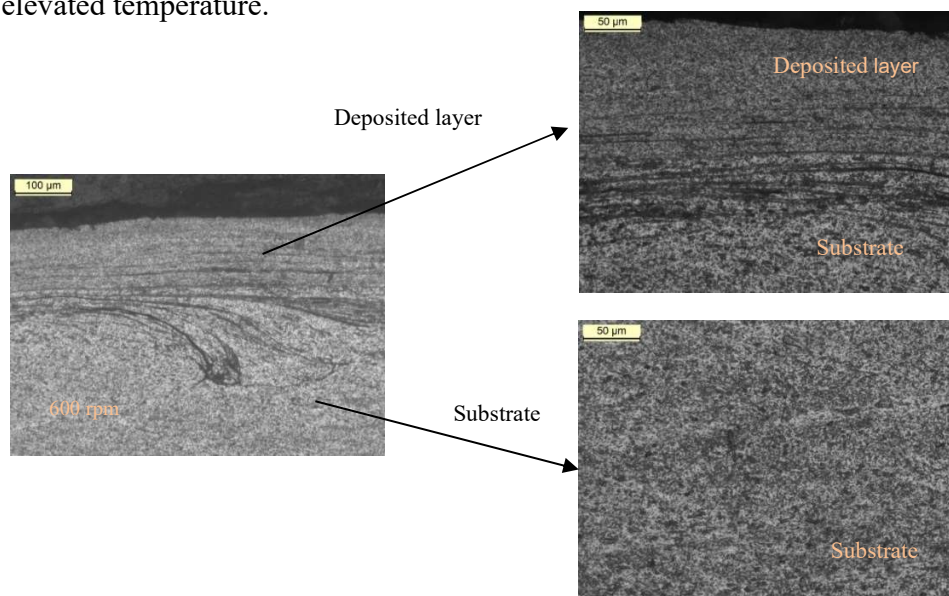


Figure 22. Comparison of microstructure between deposited layer and substrate.

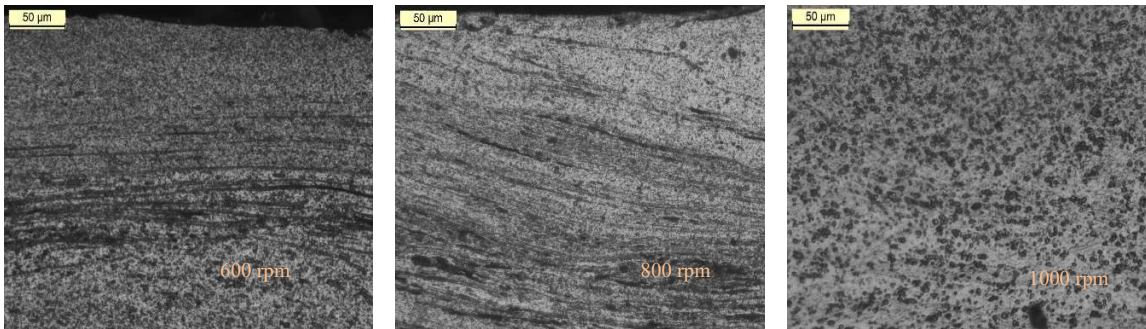
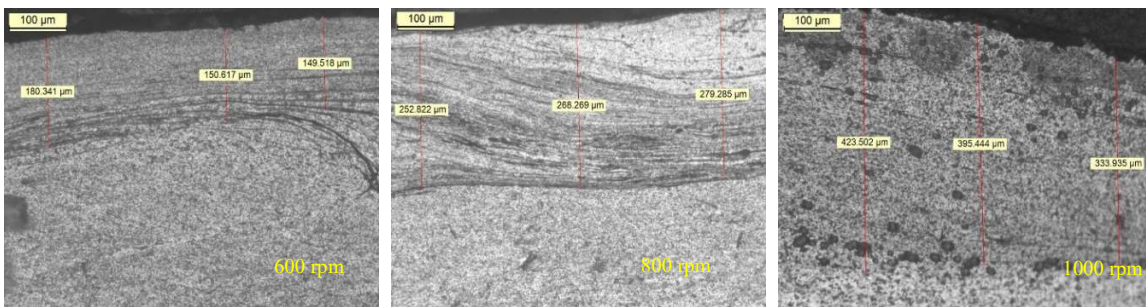


Figure 23. Comparison of microstructure at different rotational speed.



Rotational Speed (rpm)	600	800	1000
Average height (μm)	160.159	266.792	384.294

Figure 24. Height of deposition at different rotational speed.

#### 2.4.6. Wear Test

To know the mechanism of wear as well as the wear resistance of surface fretting wear was performed. Fretting wear is destructive phenomenon that occurs between two contacting surface having oscillatory motion of small amplitude. One of the most important effect of fretting wear is its contribution to fatigue failure and therefore should be studied for the quality of deposition (Geitner & Bloch, 2012). The important factors that influence the fretting wear are the load, frequency, duration, temperature, humidity, surface finish and lubricants. The test was performed under load of 5 N with a frequency of 25 Hz for time duration of 15 minutes. The wear rate of the deposition increased with the increasing rotational speed as shown in figure 19. The reason being the decreasing value of hardness

with increasing rotational speed (Geitner & Bloch, 2012). The coefficient of friction vs rotational speed curve although was not monotonous but showed a downward slope of trend line as shown in figure 26 mainly because coefficient of friction depends on many factors along with hardness. The SEM analysis showed different mechanism of wear namely, adhesive wear and abrasive wear. The EDX analysis of wear track showed no presence of oxygen coating in form of alumina which is major problem associated with fusion based AM processes.

Table 10. Fretting wear test.

Rotational speed (rpm)	Wear Rate mm <sup>3</sup> /min	Coefficient of friction (μ)
600	7.44	0.83
700	12.32	1.14
800	50.81	0.90
900	172.87	0.97
1000	222.22	0.82
Base material	98.77	0.78

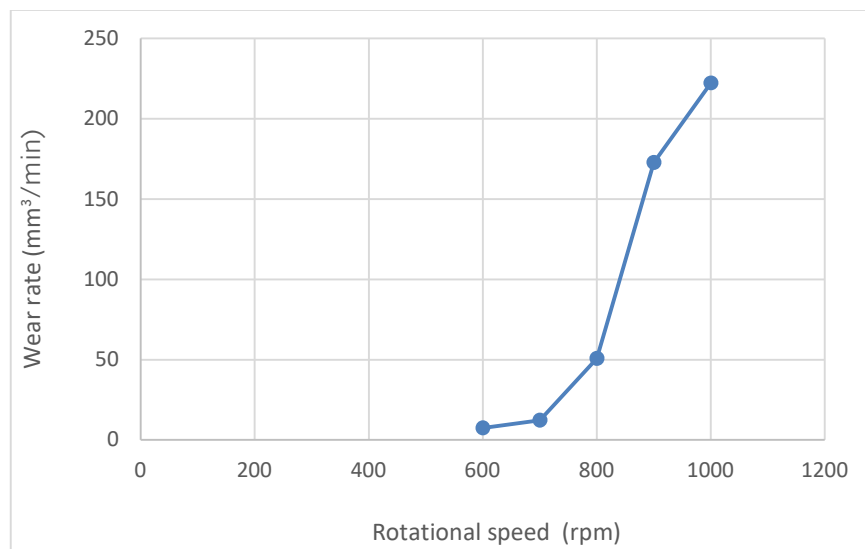


Figure 25. Graphical representation of wear test

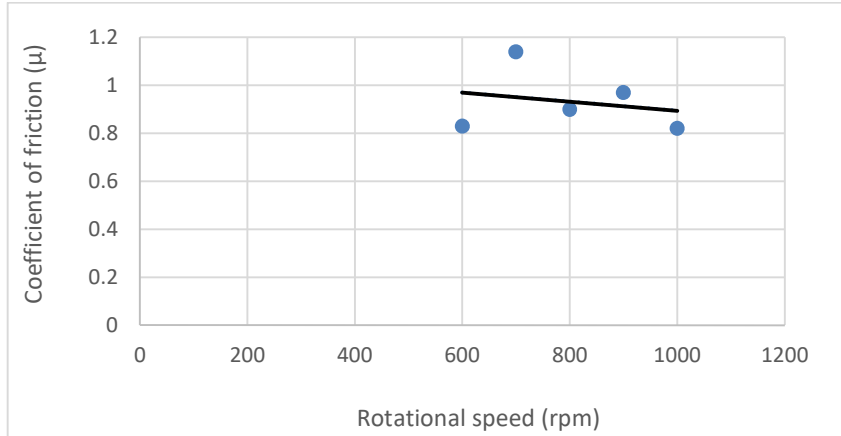


Figure 26. Coefficient of friction vs rotational speed.

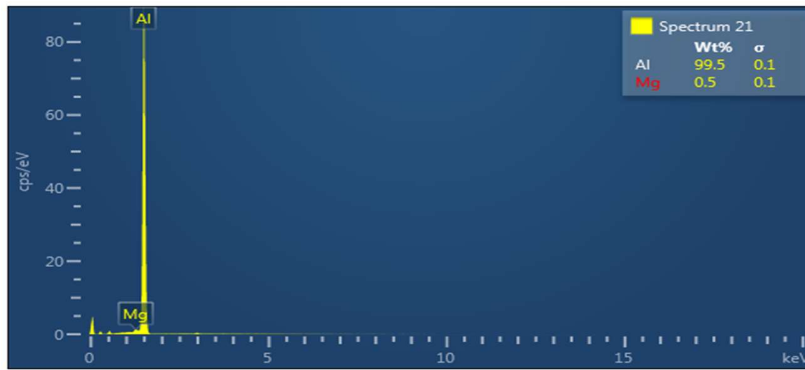


Figure 27. EDX analysis of wear track.

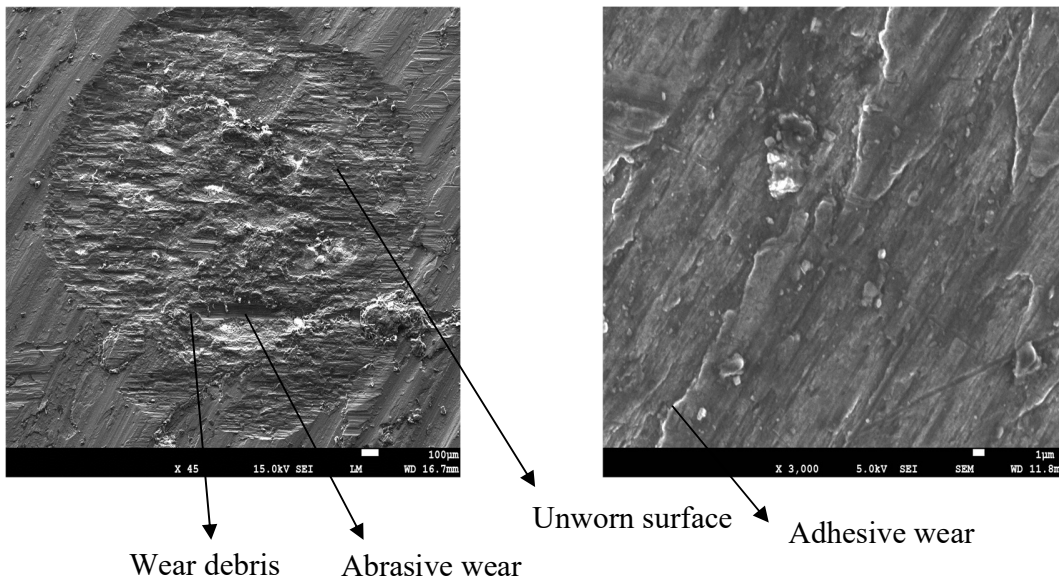


Figure 28. SEM of wear track.

#### 2.4.7. Surface Roughness Test

Surface roughness is a measure of micro-irregularities on the surface texture and consist of three components, namely roughness, waviness and form (Comprehensive material finishing, 2017). It influence surface features such as macroscopic contact angle (Hebbar, Isloor, & Ismail, 2017) , coefficient of friction, wear rate. Irregularity present on surface may form nucleation site for crack or corrosion and therefore needs to be addressed. The measurement of surface roughness involves the division of length of profile known as traversing length into parts of equal length known as sampling length. The average of the deviation from nominal surface is calculated to measure the roughness.

The surface roughness of the current deposition decreased on increasing the rotational speed because of higher heat input and better flow of material.

Table 11. Surface roughness test.

Sample number	Rotational speed (rpm)	Surface roughness ( $\mu\text{m}$ )
1	600	3.9
2	700	2.9
3	800	2.6
4	900	2.4
5	1000	2

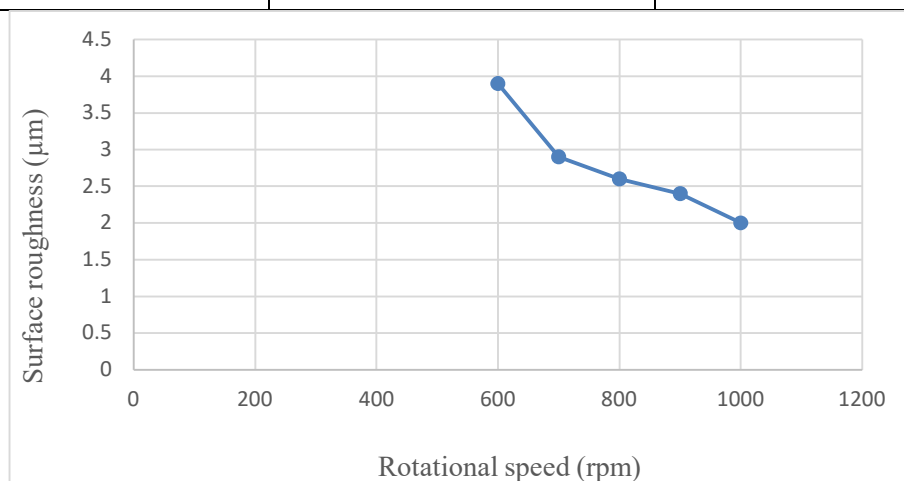


Figure 29. Surface roughness vs rotational speed.



## Chapter 3. Conclusions

In this report process parameters of two process were addressed, namely friction stir welding and friction stir powder additive manufacturing in order to characterize the weld and deposition respectively. The two process although were very different but the cause for the enhancement of mechanical properties was same i.e., dynamic recrystallization.

In the case study 1, the friction stir welding was successfully used to weld two dissimilar aluminium alloys, 6061 and 5083. Based on post welding analysis following conclusions can be made -

1. The tensile strength of the friction stir welded specimen is high compared to the fusion based welding process.
2. The grain structure in the weld zone were finer and equiaxed compared to the base material as shown by the results of optical microscopy of the welded specimen. This homogenous and finer grain structure emphasize the presence of dynamic recrystallization.
3. There is no monotonous relation between the process parameters (rotational speed and transverse speed) and mechanical strength due to complex mechanism followed during weld.
4. The combination of rotational and transverse speed should be carefully chosen to ensure the proper flow of material around the pin in order to reduce the probability of defects.
5. The results of comparison between the coolants showed that a better coolant employed during welding will yield a weld with superior mechanical properties.

In case study 2, the FSPAM was used to deposit the powder from a rotating tool on similar substrate. Based on the results of characterization following inference can be made -

1. There is was a monotonous decrease in the micro-hardness of the deposition with increasing rotational speed and the maximum micro-hardness value was nearly 174% of micro-hardness of the base material.

2. The results of the optical microscopy showed the finer, homogenous grain structure present in deposition layer compared to substrate mainly because of dynamic recrystallization.
3. The wear rate increased immensely on increasing the rotational speed with maximum value being 225 % of the wear rate of base material while the minimum was merely 7.5 % of the base material.
4. The SEM analysis showed the presence of different wear mechanisms such as abrasive wear and adhesive wear. The EDX analysis showed no presence of any kind of oxygen or alumina and hence no formation of oxide coating which is a main problem associated with fusion-based AM processes.
5. The deposition with increasing rotational speed resulted in better surface quality with smoother deposition but inferior mechanical properties such as wear rate and hardness.

## Chapter 4. Scope for Future Work

The frictional welding has been through much development in decade but still requires following areas to be explored –

1. Among various process parameters only the transverse speed, rotational speed and coolant was addressed while other parameters such as tilt angle, tool design which involves the size of shoulder and pin and the various shoulder features as addressed previously should also be studied in order to improve the performance of the weld.
2. Other coolants can also be used to further boost the efficiency of the weld.
3. The failure mechanism of the friction stir weld is another area that require much work and can be understood by analyzing and classifying the defects.
4. It could be interesting to consider the study of characteristics of weld in under water condition (hyperbaric welding).

There are some ideas I would have liked to try during the study of characteristics of deposition using FSPAM so as to fully able to predict the performance of manufactured component. The following ideas could be tested-

1. The present study only focused on rotational speed but the influence of other parameters such as transverse speed, tilt angle, powder flow rate cannot be neglected and could be investigated.
2. It would have been interesting to try tools with different shoulder features in order to study its impact on uniformity and other properties of deposition.
3. The gas in the present experiment was supplied to the powder feeder at the top but a modification can be tried in which the supply will be attached to the collet of the FSPAM setup so as to further increase the powder flow rate.
4. In the present study we have used the gas as carrier for powder but a forced feeding method can be employed using auger screw so as to increase the efficiency of powder feeder.



## References

1. Arbegast, W. J. (2006). Friction stir welding after a decade of development. *Welding Journal*, 85(3), 28–35.
2. Dawes, C. J., & Thomas, W. M. (1996). Friction stir process welds aluminium alloys. *Welding Journal*, 75(3), 5–41.
3. Feng, Z., Wang, X. L., David, S. A., & Sklad, P. S. (2007). Modelling of residual stresses and property distribution in friction stir welds of aluminium alloy 6061-T6. *Science and Technology of Welding and Joining*, 12(4), 348–356.
4. Fraser, K., St-Georges, L., & Kiss, L. I. (2016). A Mesh-Free Solid-Mechanics Approach for Simulating the Friction Stir-Welding Process. *Joining Technologies*.
5. Geitner, F. K., & Bloch, H. P. (2012). Metallurgical Failure Analysis. In *Machinery Failure Analysis and Troubleshooting*.
6. Hebbar, R. S., Isloor, A. M., & Ismail, A. F. (2017). Contact Angle Measurements. In *Membrane Characterization*.
7. Khan, N. Z., Siddiquee, A. N., Khan, Z. A., Bajaj, D., & Ubaid, M. (2018). Understanding the dissimilar friction stir welding through force and temperature evolution. *Materials Today: Proceedings*, 5(9), 17125–17131.
8. Khodabakhshi, F., & Gerlich, A. P. (2018). Potentials and strategies of solid-state additive friction-stir manufacturing technology: A critical review. *Journal of Manufacturing Processes*, 36(July), 77–92.
9. Mahto, R. P., Bhoje, R., Pal, S. K., Joshi, H. S., & Das, S. (2016). A study on mechanical properties in friction stir lap welding of AA 6061-T6 and AISI 304. *Materials Science and Engineering A*, 652, 136–144.
10. Mishra, R. S., & Ma, Z. Y. (2005). Friction stir welding and processing. *Materials Science and Engineering R: Reports*, 50(1–2), 1–78.
11. Ni, Y., Fu, L., Shen, Z., & Liu, X. C. (2019). Role of tool design on thermal cycling and mechanical properties of a high-speed micro friction stir welded 7075-T6 aluminum alloy. *Journal of Manufacturing Processes*, 48(September), 145–153.
12. Peel, M., Steuwer, A., Preuss, M., & Withers, P. J. (2003). Microstructure, mechanical properties and residual stresses as a function of welding speed in

- aluminium AA5083 friction stir welds. *Acta Materialia*, 51(16), 4791–4801.
13. Rathee, S., Srivastava, M., Maheshwari, S., Kundra, T. K., & Siddiquee, A. N. (2018). Friction Based Additive Manufacturing Technologies. In *Friction Based Additive Manufacturing Technologies*.
  14. Rivera, O. G., Allison, P. G., Jordon, J. B., Rodriguez, O. L., Brewer, L. N., McClelland, Z., ... Hardwick, N. (2017). Microstructures and mechanical behavior of Inconel 625 fabricated by solid-state additive manufacturing. *Materials Science and Engineering A*, 694(October 2016), 1–9.